

AV Nodal Function During Atrial Fibrillation: The Role of Electrotonic Modulation of Propagation

FRITS L. MEIJLER, M.D., JOSÉ JALIFE, M.D.,* JACQUES BEAUMONT, Ph.D.,*
and DHANANJAY VAIDYA*

From the Heart-Lung Institute, University of Utrecht, Utrecht, The Netherlands; and the *Department of Pharmacology, SUNY Health Science Center at Syracuse, Syracuse, New York

AVN Function in Atrial Fibrillation. The irregular ventricular rhythm that accompanies atrial fibrillation (AF) has been explained in terms of concealed conduction within the AV node (AVN). However, the cellular basis of concealed conduction in AF remains poorly understood. Our hypothesis is that electrotonic modulation of AVN propagation by atrial impulses blocked repetitively within the AVN is responsible for changes in function that lead to irregular ventricular rhythms in patients with AF. We have tested this idea using two different simplified computer ionic models of the AVN. The first ("black-box") model consisted of three cells: one representing the atrium, another one representing the AVN, and a third one representing the ventricle. The black-box model was used to establish the rules of behavior and predictions to be tested in a second, more elaborate model of the AVN. The latter ("nine-cell" model) incorporated a linear array of nine cells separated into three different regions. The first region of two cells represented the atrium; the second region of five cells represented the AV node; and the third region of two cells represented the ventricle. Cells were connected by appropriate coupling resistances. During regular atrial pacing, both models reproduced very closely the frequency dependence of AV conduction and refractoriness seen in patients and experimental animals. In addition, atrial impulses blocked within the AV node led to electrotonic inhibition or facilitation of propagation of immediately succeeding impulses. During simulated AF, using the nine-cell model, random variations in the atrial (A-A) interval yielded variations in the ventricular (V-V) interval but there was no scaling, i.e., the V-V intervals were not multiples of the A-A intervals. As such, the model simulated the statistical behavior of the ventricles in patients with AF, including: (1) the ventricular rhythm was random; and (2) the coefficient of variation (standard deviation/mean) of the ventricular rhythm was relatively constant at any given mean V-V interval. Analysis of cell responses revealed that repetitive atrial input at random A-A intervals resulted in complex patterns of concealment within the AVN cells. Consequently, the effects of electrotonic modulation were also random, which resulted in a smearing of the AV conduction curve over A-A intervals that were larger than those predicted for 1:1 AV conduction. Hence, during AF, electrotonic modulation acts in concert with the frequency dependence of AVN conduction to result in complex patterns of ventricular activation. Finally, similarly to what was shown in patients, VVI pacing of the ventricle in the nine-cell model at the appropriate frequency led to blockade of nearly all anterograde (i.e., A-V) impulses. The essential feature here was that the retrograde impulse invading the AVN cells was followed by refractoriness with slow recovery of excitability, setting the stage for electrotonic inhibition of anterograde impulses. Overall, the results provide insight into the cellular mechanisms underlying AVN function and irregular ventricular response during AF. (*J Cardiovasc Electrophysiol*, Vol. 7, pp. 843-861, September 1996)

concealed conduction, electrotonic modulation of AV conduction, irregular ventricular rhythm

Supported in part by Grants P01-HL39707 and R01-HL29439 from the National Heart, Lung, and Blood Institute of the National Institutes of Health, and by a grant from the Whale ECG Foundation.

Address for correspondence: José Jalife, M.D., Department of Pharmacology, SUNY Health Science Center at Syracuse,

766 Irving Avenue, Syracuse, NY 13210. Fax: 315-464-8000.

Manuscript received 24 January 1996; Accepted for publication 20 May 1996.

Introduction

The relatively slow irregular ventricular rhythm that accompanies atrial fibrillation (AF) has been explained in terms of repetitive concealment of electrical impulses of atrial origin within the AV node (AVN), as a result of decremental conduction.^{1,2} This concept was challenged by the postulate that the ventricular rhythm in patients with AF could be more easily explained by electrotonic modulation of AVN pacemaker activity.^{3,4} However, several objections have been put forth against the latter conjecture. For instance, it is difficult to escape the argument that, during rapid atrial rhythms, AVN pacemaker activity might be overdrive suppressed by the rapidly incoming impulses of atrial origin. This has led us to reevaluate the above hypotheses and to propose that neither decremental conduction nor pacemaker activity within the AVN need, in fact, be involved in the mechanism(s) responsible for the rate and rhythm of the ventricular response during AF. Our postulate is that continual electrotonic modulation of AVN propagation may be used to explain most, if not all, of the phenomena that have been described in relation to the ventricular responses during AF. Indeed, it remains our contention that the idea of decremental conduction is incompatible with: (1) the known electrophysiologic properties of the AVN; and (2) a number of electrocardiographic features observed in patients with AF.

We further believe that it is more appropriate to think of the AVN as an area of electrical discontinuities whose safety factor for propagation is relatively small.^{5,6} Under these conditions, frequency-dependent AVN propagation patterns during supraventricular tachyarrhythmias may be readily explained in terms of electrotonically mediated inhibition⁷ and/or facilitation of the activation of cells in the AVN. The concept of electrotonic modulation of propagation^{7,8} is a viable and realistic alternative to the original ideas of decremental conduction or electrotonic modulation of pacemaker activity in explaining ventricular rate and rhythm during AF.

In this article, we will first review the hypotheses that have been postulated to explain the cellular bases of various phenomena associated with AVN conduction during AF. We will then present the results of computer simulations using simplified models of AVN function during AF. The models make use of the ideas of electrotonic modulation of propagation as being the mechanism of concealed AVN conduction during AF.

Concealed Conduction

It has been known for many years that an impulse entering the AVN can sometimes fail to traverse it completely.⁹ In 1948, Langendorf¹⁰ first used the term "concealed conduction" to describe such a phenomenon, whose diagnosis is based on the presence of incomplete conduction coupled with an unexpected behavior of the subsequent impulse.¹¹

Initially, Langendorf¹⁰ restricted the use of the term as follows: (1) to explain partial or incomplete forms of anterograde and/or retrograde AV conduction block in which a proximal (i.e., atrial or ventricular) impulse did not generate a distal response but had an influence on impulses that followed it; and (2) to indicate "abortive" AV conduction of a premature junctional impulse blocked in both directions and causing first- or second-degree AV block. Over the years, the list of applications of the concept of concealed conduction has grown substantially to include, among others, the explanation for the relatively slow irregular ventricular rhythm during AF. The concept of concealed conduction states that the ventricular rhythm is determined by such conditions as strength, form, number, direction, and sequence of the fibrillatory impulses that reach the AVN from the atrium, and by the electrophysiologic properties of the AVN.^{12,13} Accordingly, the long R-R intervals during AF are a consequence of repetitive concealed anterograde AVN conduction, while the shortest R-R intervals represent the functional refractory period of the AVN.^{2,14}

Decremental Conduction Versus Discontinuous Propagation

Decremental conduction has been almost universally accepted as the most likely mechanism responsible for the characteristic slowing of conduction and block associated with repetitive premature excitation of the AVN. The idea derives from the original studies of Hoffman,¹⁵ who concluded that the AVN was the site for slow but continuous conduction of electrical impulses from the atrium to the His bundle. As the impulses travel across the center of the node, a progressively increasing threshold, a decreasing space constant, and a decreasing amplitude and rate of rise of the action potentials would lead to a gradual decay of the effectiveness of the active regions to depolarize more distal tissues. Accordingly, block can occur if the area of decremental conduction is sufficiently long. This concept was used by Paes

de Carvalho and de Almeida¹⁶ to explain their recordings of Wenckebach block in an "NH" cell of the isolated rabbit AVN. Stimulation of the atrium at a constant cycle length demonstrated progressively increasing delay in transmission across an impaled AVN cell (their Fig. 4). However, a close look at their figure clearly reveals that there are no major changes in the upstroke of the action potentials that can account for the progressive delay, except for the fact that the electrotonic foot of the superimposed active responses follows a time course that is practically the same as that of the subthreshold response evoked by the blocked impulse.

It is important to note that decremental conduction as conceptualized by Hoffman¹⁵ can occur only in homogeneous and continuous excitable media. This is clearly not the case for the AV conducting system, which is highly heterogeneous and discontinuous. Moreover, several years ago, Zipes, Mendez, and Moe¹⁷ pointed out that, because of discreteness of cell-to-cell connections in the AVN, the phenomenon observed by Paes de Carvalho and de Almeida¹⁶ could be readily explained in terms of electrotonically mediated delay of activation. Decremental conduction of an impulse differs from electrotonic transmission into an unexcitable fiber in that, in decremental conduction, the amplitude of the active response (i.e., the action potential) decreases gradually until it dissipates completely, being unable to excite tissue ahead of it, while in electrotonic transmission, the action potential stops at the site of block. The local circuit currents generated, induce "passive" membrane depolarization whose amplitude decays with distance and as a function of the resistive properties of the tissues involved. To our knowledge, there is no evidence in the relevant literature that provides definite support to the idea that conduction through the AVN is, in fact, decremental, and studies on AVN propagation patterns in response to influences that inhibit AVN propagation, such as cholinergic stimulation, have failed to confirm it.¹⁸ In fact, recent studies in the isolated AVN of the rabbit¹⁹ have shown that cholinergic activity leads to complex patterns of AVN activation that would be difficult to explain in terms of decremental conduction.¹⁹ Moreover, considerable evidence has been accumulated in support of the idea that electrotonic modulation of propagation may be associated with delayed recovery of excitability in the AVN. For example, Billette²⁰ carried out an extensive mapping study of the mechanism of cycle-length-dependent AVN conduction delay.

This author demonstrated that with shortening of the cycle length, action potentials in the N zone dissociated progressively into two components, similar to those shown by Paes de Carvalho and de Almeida¹⁶ during acetylcholine superfusion. This indicates that during successful propagation in each case, the impulse actually ceases being an active depolarization at some point proximal to the impaled cell. The mechanism proposed was similar to that described for discontinuous propagation in other tissues, where an unexcitable segment interposed between two excitable regions functions as a purely passive resistance-capacitance circuit.^{6,21} Blockade of the impulse is due to cessation of active transmission at the unexcitable element. Propagation can be caused by electrotonic current bringing distal excitable cells to threshold. The key condition for such a mechanism in AVN transmission is, therefore, that a nodal cell must become functionally unexcitable at short cycle lengths. Indeed, it is well known that in the AVN, the recovery of excitability outlasts the action potential duration,²² which may be crucial for explaining failure of premature or successive rapid impulses to propagate through the AVN. As the impulse becomes more premature, the wavefront initiated proximal to the AVN encounters less recovered nodal cells, until the electrotonically initiated depolarization is incapable of reaching threshold level and block occurs.⁶

In their recent article, Watanabe and Watanabe¹ strongly advocated the concept of decremental conduction to challenge the postulate of Meijler et al.^{4,23} on the role of electrotonic modulation of pacemaker activity during AF. The Watanabes have postulated that in AF, "AV block occurs because of decremental conduction rather than by a refractory barrier, although the resultant concealed conduction would prolong the refractory period of distant nodal fibers and further modify the conduction pattern." Subsequently, in the same article, they proposed that decreases in the upstroke velocity (V_{max}) of the AVN action potential, secondary to decreases in i_{Ca} , could possibly explain the occurrence of frequent concealment in the N region "even after the expiration of its effective refractory period."¹ There are two major problems with such speculations. The first one relates to the idea that decremental conduction and block within the AVN can occur, irrespective of the timing of the atrial impulse. Indeed, a close look at the theoretical ladder diagram presented in their Figure 3B shows that, for unexplained reasons, the third atrial impulse is blocked high in the AVN, despite

the fact that it arrives appreciably later than the second atrial impulse. It would be impossible to account for blockade high in the AVN under such conditions, even if the mechanism of blockade were a gradual decrease in V_{max} . The second and more important problem is that Watanabe and Watanabe¹ do not consider any possible after-effects (electrotonic or otherwise) that the concealed impulse may have on subsequent impulses. Again, analysis of their Figure 3B reveals that the fifth impulse, which is supposed to be concealed, does not seem to have any effect on the sixth impulse, which conducts normally. Thus, as we indicated at the outset, although electrotonic modulation of pacemaker activity may not explain some of the phenomena associated with the AVN response to AF, the explanation of Watanabe and Watanabe,¹ based on the concept of decremental conduction, seems at least equally unsatisfactory. As we shall demonstrate below, the concept of electrotonic modulation of propagation can more readily account for the behavior of the AVN during AF.

Electrotonic Modulation and Concealed Conduction

When an impulse initiated in the atria or ventricles is blocked within the AVN, it is clear that the depolarization induced by that impulse may be subthreshold for cells just distal to the site of block. This subthreshold event is the result of electrotonic current flow from depolarized to nondepolarized cells, which may be manifest at appreciable distances ahead of the site of block, and can be demonstrated using microelectrode recordings of AVN action potentials during the application of premature stimuli.²⁴ It has been shown that electrotonic depolarizations can have profound effects on the electrophysiologic properties of the tissue distal to the block.^{25,26} Antzelevitch and Moe⁷ used two different models of isolated cardiac Purkinje fibers to demonstrate that electrotonic depolarizations can produce delay or even blockade in the transmission of subsequent impulses, depending on time relations. They used the term "electrotonic inhibition" to describe this phenomenon and suggested that many published clinical examples of concealed conduction may be explained in terms of electrotonic inhibition of excitability. Inhibition of excitability by subthreshold stimulation has been demonstrated in human hearts.²⁷ In addition, Oreto et al.²⁸ interpreted a clinical electrocardiographic case of exit block from an idioventricular pacemaker as being the result of electrotonic inhibition

by conducted impulses of supraventricular origin. It has also been proposed that electrotonic inhibition may prevent ventricular fibrillation during AF,²⁹ and the concept has been used also to explain functional inexcitability in the center of vortices of reentrant activity.³⁰

Recently, Davidenko et al.³¹ demonstrated electrotonic inhibition of excitability in single ventricular myocytes under current clamp conditions. Application of repetitive depolarizing pulses of threshold amplitude elicited action potentials in a 1:1 manner. Interpolation of single brief subthreshold pulses during individual diastolic intervals led to transient decays in excitability and even complete failure of subsequent excitation. Such results are in full agreement with the data obtained previously by Antzelevitch and Moe⁷ in multicellular preparations. More recently, Liu et al.⁸ carried out current and voltage clamp experiments in single, enzymatically dispersed, myocytes from the rabbit AVN, as well as computer simulations, to study the ionic mechanisms of electrotonic inhibition and to determine the cellular basis of concealed AVN conduction. Voltage clamp analysis in both experiments and simulations demonstrated that electrotonic inhibition was the result of partial inactivation of the transient calcium current ($I_{Ca,T}$). In addition, Liu et al.⁸ demonstrated that the ability of the subthreshold response to prevent subsequent excitation of an AVN cell was increased when the interval between the conditioning subthreshold pulse and the succeeding pulse was shortened, or when the amplitude of the subthreshold pulse was increased. Moreover, they simulated AVN propagation using a linear array of "AV nodal" cells and demonstrated that when a premature impulse failed to traverse the AVN, the subthreshold depolarization elicited downstream of the site of block led to a transient reduction of excitability, with consequent delay or block of the following impulse. Such results have provided the strongest evidence to date in support of the idea that at least some of the manifestations of concealed AVN conduction can be the result of electrotonic inhibition secondary to a transient decrease in $I_{Ca,T}$.

Discontinuous AVN Propagation: A "Black-Box" Approach

The concept of discontinuous AVN propagation provides an excellent framework for the understanding of the mechanisms of various electrocardiographic manifestations of concealed AV con-

duction. Let us consider the oversimplified “black-box” model of AV conduction shown in Figure 1. The model is composed of a linear but heterogeneous array of three excitable elements, each described by an ionic model of a cardiac cell. Element 1 represents the atrium (A); element 2 represents the AVN; and element 3 represents the ventricle (V). The equations used for the atrial and ventricular cells were modified from those in the Luo and Rudy³² model. The equations used for the AVN cell were similar to those used by Liu et al.⁸ Tables 1 and 2 show the currents used for each model, as well as the maximal conductances and reversal potentials. The AVN has a higher intracellular resistance and lower upstroke velocity and, therefore, conducts slower than the other two. The electrophysiologic properties of A and V are similar to each other, except that A has a briefer action potential duration than V. The cells are arranged end to end and connected by coupling resistances (25 k Ω) that are higher than the intracellular resistance of each cell. In this system, impulse propagation will occur in such a way that after stimulation of A, depolarization reaches threshold and supplies electrotonic current for AVN, which fires after a small but discrete interval (see arrow). The AVN cell in turn provides depolarizing electrotonic current to bring V to threshold (arrow) for its action potential. Thus, in this system, conduc-

tion is stepwise with the electrotonic currents propagating from cell to cell, to initiate at each step a local “all or none” action potential. If one were to extrapolate the behavior of such a system to the real-life situation, one could say that the activity generated in the AVN by impulses traveling from the atria or ventricles propagates through local circuit (i.e., electrotonic) currents. Such propagation leads to stepwise and discontinuous local excitation even though, at the macroscopic level, cell-to-cell excitation appears to be continuous, particularly at relatively slow heart rates. Discontinuous AVN propagation may become manifest at very fast heart rates or during premature antero- or retrograde propagation.

In the black-box model described above, discontinuous propagation is the result of the varying intracellular and intercellular resistances. Similarly, in the real-life situation, discontinuous propagation is the result of structural and electrophysiologic heterogeneities along the AV transmission system, including differing cell geometries and variable three-dimensional arrangements of cell-to-cell connections.³³ However, a more important source of heterogeneity is provided by the large structural and electrophysiologic differences that exist in the various types of AVN cells.³⁴ Discontinuous propagation may become manifest at the junctions between regions when heart rate is increased. For

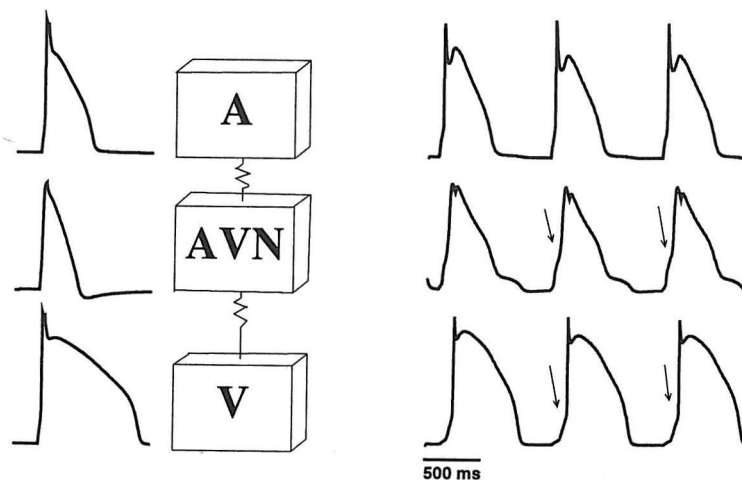


Figure 1. “Black-box” model of the AV node consisting of three cells coupled by passive resistances. The individual action potentials of the atrial (A), AV nodal (AVN), and ventricular (V) cells are displayed on the left side. The right side shows the conduction of impulses from the atrial to the ventricular cells; the arrows point to the electrotonic “foot” and show the time lag between action potentials. The ventricular and atrial action potentials were reconstructed using equations modified from the Luo and Rudy model.³² The equations for the AV nodal action potentials were similar to those of Liu et al.⁸ The model equations were integrated using a semi-implicit backward Euler integration scheme.⁵⁷ We used a time step of 50 μ sec and an error tolerance on the membrane potential of 0.01 mV. In all simulations using the three-cell model, coupling resistance was 25 k Ω .

TABLE 1
Currents Used for Atrial and Ventricular Cells

Current	Reference	Atrium \bar{g} (ms/cm ²)	Ventricle \bar{g} (ms/cm ²)	E _{rev} (mV)
I _b (background)	32	0.03921	0.03921	-59.8
I _{Na} (sodium)	32	23.0	23.0	54.4
I _{si} (slow inward)	32	0.09	0.09	80.0
I _K (delayed rectifier)	54	70.0	9.0	-78.0
I _{Kp} (plateau potassium)	32	*	*	-87.9
I _{K1} (inward rectifier)	32	*	*	-87.9

* Value depends on membrane potential.

example, to reach the ventricle, an impulse originated in the atrium has to propagate across the various regions of the AVN (e.g., AN, N, and NH regions), and then through the His-Purkinje network. Such an impulse must therefore travel across junctions between several areas that have varying electrophysiologic properties, including excitability, cell-to-cell coupling, and refractoriness. Thus, as in our simplified black-box model (Fig. 1), a premature impulse generated in the atria or ventricles may reach a junction (e.g., atrium-node, node-His bundle) in which propagation is not possible because the tissue has not yet recovered. The impulse may stop at this point and become extinguished, or it may renew its journey, but only after a delay imposed by the amplitude of the electrotonic signal and by the time necessary for the recovery of excitability of the cells distal to the site of block.

Electrotonic Modulation of Propagation

In an effort to understand AVN function during AF, we use the black-box approach described above. This implies that the electrical processes that take place inside the AVN during propagation are inferred from what is measured at either side of the box. We are, of course, well aware that this model represents a gross oversimplification of the AV transmission system and that it does not take into consideration the structural and electrophysiologic complexities of the various cell-regions involved. Yet, as we shall demonstrate below, even a simple black-box model can help to understand the sometimes perplexing behavior of the AVN during AF. Clearly, many years of experience in deductive electrocardiology have shown that simple conceptual models may be quite useful, even when most of the elements of the system are hidden from view.

Model Requirements

Any model that simulates the behavior of the ventricles in AF must fulfill the following statistical conditions:

- (1) The ventricular rhythm should be random.¹²
- (2) The coefficient of variation (CV = standard deviation/mean) of the atrial intervals during AF should be constant and independent of the number of atrial depolarizations/per unit time.³⁵
- (3) Similar to the CV of the atrial rhythm, the CV of the ventricular rhythm during AF should also be constant and independent of the number of atrial or ventricular depolarizations per unit time.^{23,35}

Validation of the Model

We have used two different mathematical models to test the hypothesis that electrotonic modulation of AVN propagation plays a major role in the phenomena that have been described in relation to the ventricular responses during clinical AF. The first model, which consists of only three cells, established the rules of behavior that must be fulfilled on the basis of well-known parameters that describe AVN function. The second, nine-cell model is used to test predictions regarding the statistical behavior expected of the ventricular rhythm during AF. First we determined the black-box model's ability to reproduce normal AVN behavior.

Frequency Dependence of AVN Conduction

The behavior of the three-cell model during basic as well as during premature atrial stimulation is shown in Figure 2. Panel a shows results obtained at a basic cycle length (i.e., A1-A1) of 1000 msec, which resulted in a steady-state A1-V1 interval of 38 msec. A premature stimulus, A2, applied after the tenth basic impulse (second A1 in the panel) at an A1-A2 interval of 403 msec

TABLE 2
Currents Used for AVN Cell

Current	Reference	\bar{g} (ms/cm ²)	E _{rev} (mV)
I _b (background)	55	*	-60
I _{bias} (bias current)	8	*	always positive
I _{si} (slow inward)	55	12.5	30
I _{Ca,T} (T-type calcium)	8	48.3	40
I _K (delayed rectifier)	56	*	-90

* Value depends on membrane potential.

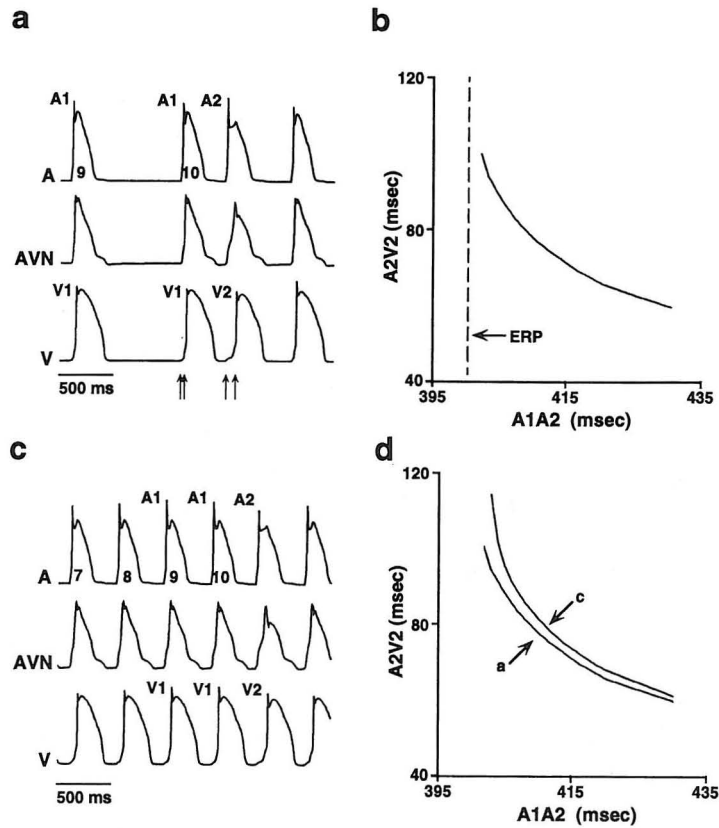


Figure 2. Frequency dependence of AV nodal function in the black-box model. The three traces in panels a and c represent the time changes in the potentials of the atrial (A), AV nodal (AVN), and ventricular (V) cells. In panel a, stimulation at a basic A1-A1 interval of 1000 msec for ten beats resulted in a constant conduction time of 38 msec (beats 9 and 10 are shown). A premature impulse at 403 msec has conduction time of 94 msec. Upward arrows indicate A-V interval. Panel b: Graph of A2V2 times plotted against varying premature A1A2 intervals. The vertical line marks the effective refractory period (ERP). Panel c: The steady-state (A1-V1) conduction time for a basic cycle length (A1-A1) of 430 msec is 61 msec (beats 7 to 10 are shown). A premature impulse (A2) at 403 msec is conducted in 114 msec. Curve c in panel d is the conduction delay curve for a basic cycle length of 430 msec. Curve a is the same as the one in panel b. Note the rightward shift of curve c.

yielded a prolonged A2-V2 interval (94 msec). Note that the short A1-A2 interval is followed by prolongation in the electrotonic foot (bracketed by upward arrows) that precedes the responses in both the AVN (second trace) and V (third trace) cells. In panel b, a complete scan of the diastolic interval with progressively earlier A2 stimuli resulted in a monotonically increasing A2-V2 conduction curve. It is clear from this plot that the effective refractory period (ERP = 400 msec), defined as the minimum A1-A2 that resulted in a propagated V response, outlasted the action potential duration of the AVN and of the V cell. Panel c shows results from a similar computation in which the basic A1-A1 interval was 430 msec. Clearly, at this cycle length the steady-state A1-V1 interval was appreciably longer (61 msec) than in panel a. In addition, application of a premature A2 stimulus at the same A1-A2 (403 msec) interval as

in panel a resulted in greater prolongation of A2-V2 (114 msec). Note again the electrotonic depolarizations that precede the active responses in AVN and V, as well as those produced by the delayed activation of the AVN cell on the atrial membrane potential. As panel d demonstrates, at the short basic cycle length (curve labeled c), the A2-V2 conduction curve is shifted to the right, with a consequent prolongation of the ERP. These results reproduce very closely the frequency dependence of slow conduction and refractoriness that is typical of AVN propagation in most patients.³⁶ In addition, the results in Figure 2 demonstrate that, in this model, slow AVN conduction is not the result of decremental but rather discontinuous propagation provided by the large intercellular resistances connecting the three cells. Obviously, from these data one can expect that during AF, random variations in the A-A inter-

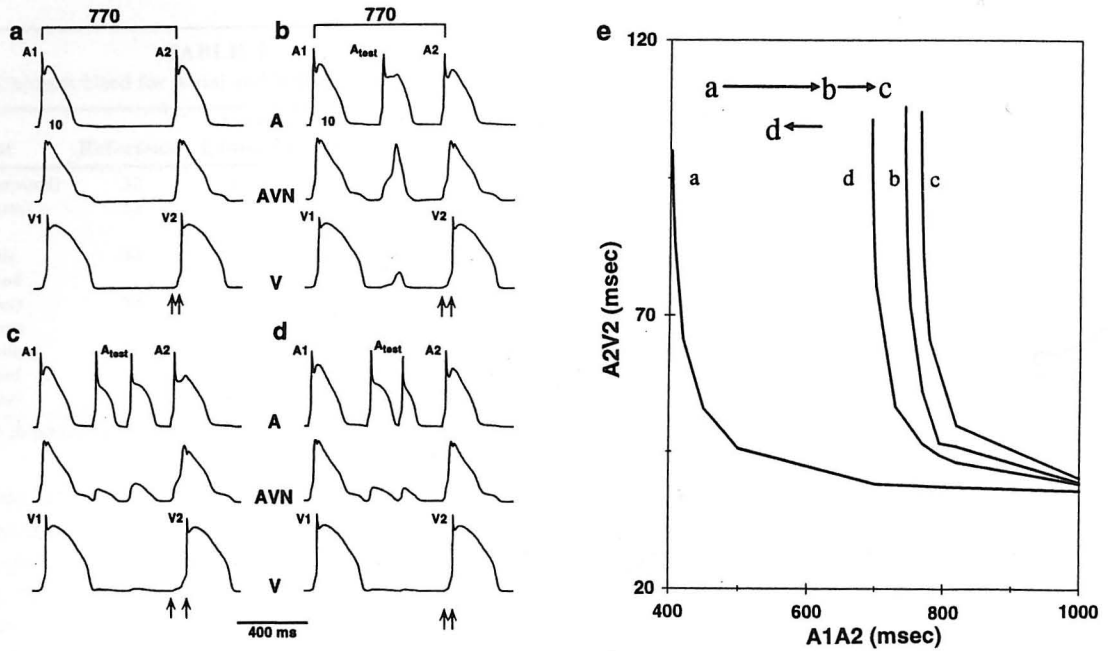


Figure 3. Effects of electrotonic inhibition and facilitation in AVN function. The basic cycle length (not shown) in panels a, b, c, and d was 1000 msec, and the steady-state conduction time was 38 msec. A2 impulses applied at a constant A1-A2 interval of 770 msec after the tenth basic response have a conduction time of 38.75 msec (panel a). Panel b: A single test pulse (A_{test}) is applied at 395 msec (blocked below the AV nodal cell); the conduction time A2V2 is 55.95 msec. Panel c: Two test pulses are applied sequentially at 320 and 520 msec. Panel d: Test pulses are applied at 340 and 520 msec. The electrotonic effects of these concealed impulses alter AVN conduction depending on time relations. The conduction times are 80.8 and 46.5 msec in panels c and d, respectively. Panel e shows shifts in conduction delay curves for each of the above protocols (curves a, b, c, and d).

val should produce beat-to-beat variations in the A-V interval, which will result in variations in the R-R interval. However, although frequency dependence of conduction and ERP is an essential determinant of ventricular excitation patterns during AF, it is not sufficient to fulfill the requirements listed above.

Electrotonic Modulation of AVN Conduction

Concealed conduction is usually manifested in the ventricular response when an impulse that penetrates the AVN, but fails to traverse completely, has some "after-effects" on the propagation of subsequent impulses.^{9,10} We have used the three-cell black-box model to determine whether such after-effects can be the result of electrotonic inhibition. Data from one such simulation are presented in Figure 3. In panel a, A2 stimuli were applied to the atrial element at a constant A1-A2 interval of 770 msec, which resulted in a 1:1 A-V propagation pattern at a constant interval of 39 msec (upward arrows). In panel b, a premature stimulus (A_{test}) was applied to the atrium at an A1- A_{test} in-

terval of 395 msec. This impulse failed to traverse the system but induced a subthreshold (electrotonic) depolarization in the V cell. Such a depolarization would not be manifest in an ECG (concealed conduction), except for the fact that AVN activation led to a transient decrease of AVN excitability and, consequently, to a slight prolongation in the A-V conduction time of the subsequent A2 impulse (55 to 95 msec). As shown in panel c, interpolation of two consecutive test pulses between two basic responses leads to more complex results,⁷ with the first AVN subthreshold response inhibiting the amplitude and, therefore, the electrotonic effects of the second AVN subthreshold response. As a result, depending on the time relations between the two test pulses, A-V conduction time of the A2 impulse may be more or less delayed than in panel b. In the specific case of panel c, the first subthreshold depolarization led to a reduction in the amplitude of the second and resulted in only a slightly larger increase in the A2-V2 conduction time compared to panel b. In panel d, abbreviation of the interval between the two test stimuli led to a further decrease in the amplitude of the

second subthreshold AVN response. Consequently, there was a decrease in the overall inhibitory effect on the succeeding propagated response. The graph in panel e summarizes the changes that would be expected in the A-V conduction curve as a result of one (curve b) or two (curves c and d) atrial impulses that are concealed within the AVN cell. Note that while a single subthreshold AVN response shifts the AV conduction curve of subsequent impulses to the right, the consequences of having two intervening subthreshold responses are more complex, with shifts in the AV conduction curve to the right (inhibition) or left (facilitation), depending on the relative timing of the electrotonically mediated effects.

The results in panels c, d, and e of Figure 3 demonstrate that when two electrotonic depolarizations occur within a single diastolic interval of the AVN cell, the amplitude of the second event is diminished as a result of inhibition produced by the first event. This suggests that when a very rapid succession of atrial inputs falls within a single AVN diastolic interval (after each AVN interval a V response would occur), as may be the case during AF, failure of the first input to propagate through that cell may lead to failure of subsequent inputs, because each subthreshold depolarization should inhibit the amplitude of its immediately following neighbor, which results in a cumulative inhibitory effect.^{37,38} This is precisely what happens in the model, as demonstrated by the traces presented in Figure 4. In panel a, introduction of a train of atrial inputs at a constant period of 200 msec resulted in concealment of many of such inputs with consequent changes in the V-V interval. In panel b, repetitive stimulation of the A cell at random A-A intervals (mean = 231.8 msec) resulted in complex patterns of concealment within the AVN cell with consequent changes in A-V and V-V intervals.

The results of a complete simulation in which we measured the changes in A-V conduction during AF are presented in Figure 5. In the top graph of panel a, we have plotted a typical A-A interval histogram used to simulate AF. In all such simulations, the arrival of the atrial input is characterized mathematically as a Poisson process. In this particular case, the mean A-A interval was 231.8 msec, and the standard deviation was 75.4 msec. This resulted in the unimodal V-V interval histogram shown in the bottom graph of panel a. The mean V-V interval was 522 msec, and the standard deviation was 118.3 msec. In panel b, we have plotted the A-V interval for each ven-

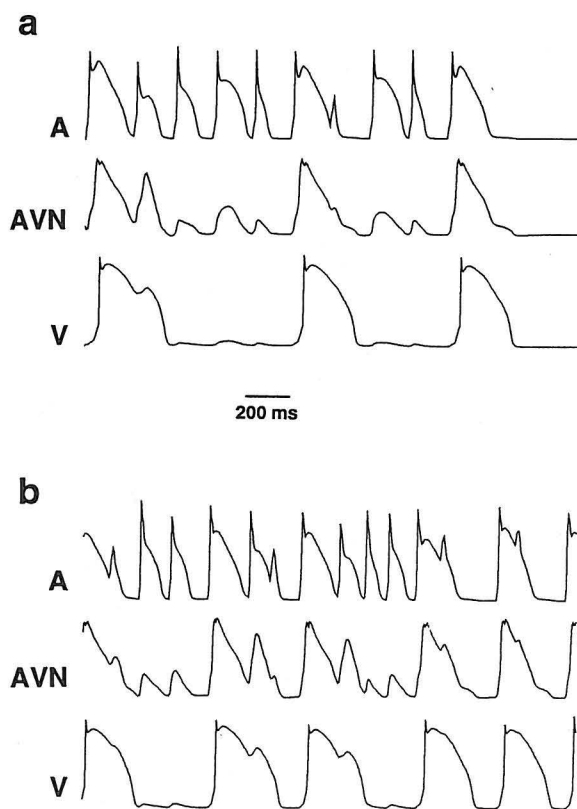


Figure 4. Panel a: Impulses at a constant period of 200 ms were input to the atrial cell (upper trace), resulting in partial transmission and concealment of many impulses in the AVN cell (middle trace), and consequent changes in V-V intervals (lower trace). Panel b: Random atrial stimuli (mean A-A = 231.8 ms) were applied. Similar changes in AVN and ventricular cells can be noted.

tricular impulse as a function of the A-A interval between successful A-V propagations. Because of the randomness of the A-A intervals, the effects of electrotonic modulation are also random, which results in a smearing of A-V intervals over A-A intervals that are larger than those predicted by the 1:1 curve.

The results presented above support the validity of the black-box model in testing the hypothesis that electrotonic modulation is the cellular basis of some of the manifestations of concealed conduction, including prolongation of A-V conduction time and the ERP for the events that follow the concealed atrial responses. The data further suggest that, during AF, these electrotonically mediated effects act in concert with the frequency dependence of A-V propagation (see Fig. 2) to result in complex patterns of A-V conduction (Fig. 5) and ventricular activation.

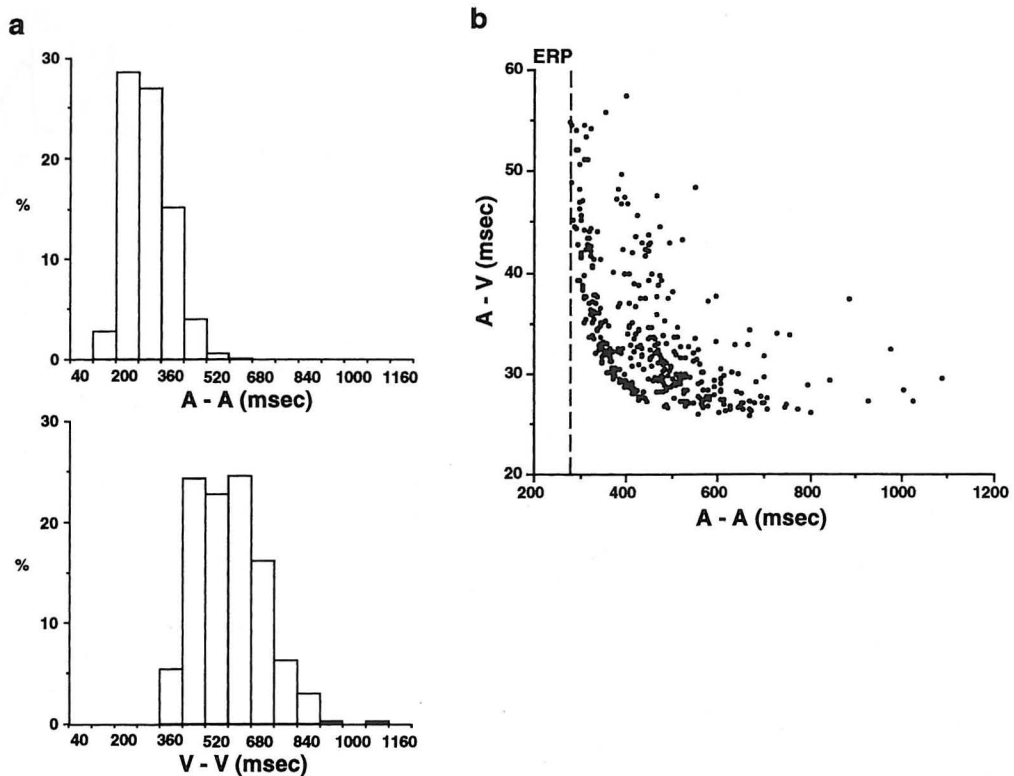


Figure 5. Panel a: The upper histogram represents the distribution of A-A intervals randomly supplied to the system (mean = 231.8 msec; standard deviation = 75.4 msec), while the lower panel shows the distribution of V-V intervals obtained (mean = 522 msec; standard deviation = 118.3 msec). Panel b: The conduction time of every successfully conducted impulse is plotted against its A-A interval (ERP = effective refractory period). Note smearing of the conduction delay curve (described in the text). "Black-box" model at a coupling resistance of 20 k Ω .

It is important to note that the model used in this study considers the AVN as a linear array of cells, which is a gross oversimplification, particularly in the presence of "dual pathway" physiology.³⁹

It is important to realize also that, in real-life AF, not only the A-A interval varies in a random fashion but probably the amplitudes and durations of the atrial impulses that reach the AVN also vary. This should result in even more complex patterns of electrotonic modulation than those shown herein.

Electrotonic Modulation and Ventricular Intervals During AF

The simulations presented in the previous section led to the following sets of rules and predictions regarding AF.

Rules

(A) Given a set of random A-A intervals (i.e., AF), the propagation of an atrial impulse may be

affected by the immediately preceding A-A interval during which A-V activation was successful (see Fig. 2).

(B) Most important, the beat-to-beat A-V interval is determined by a complex interplay between electrotonic inhibition and facilitation, induced by the multiple randomly occurring atrial depolarizations that become subthreshold in the AVN cell (see Figs. 3 and 4).

(C) Consequently, within limits dictated by the A-V propagation curve (see Fig. 5b), the ERP of the A-V transmission pathway varies randomly with the preceding successful interval between atrial impulses, and with the number and timing of concealed atrial impulses that fall between two successfully propagated ventricular responses.

(D) Similarly, the duration of the AVN functional refractory period (FRP), defined as the minimum V-V interval, is not fixed but varies randomly in accordance with the variations in the timing of atrial inputs into the node.

(E) Whether or not an atrial impulse causes AVN excitation should depend on the quality of that im-

pulse and on its timing in relation to the AVN propagation curve.

Recall that in this model, all random processes associated with A-V propagation are the result of the stochastic nature of the atrial input during AF. It is important also that the above rules are derived from simulations using an oversimplified model in which all intervals can be rigorously defined and measured. This is not the case for AF in real life. Thus, the following predictions, while directly testable in the model, will be difficult to prove in experimental or human studies, at least for the time being.

Predictions

(A) As a result of electrotonic modulation, i.e., inhibition, the probability of AVN blockade during AF should increase with an increase in the frequency of atrial impulses entering the AVN cell. Thus the mean V-V interval should increase when the mean A-A interval is decreased.

(B) During AF, the V-V intervals should change randomly, but their distribution should be independent of the distribution of the random A-A interval. In other words, because of randomly occurring electrotonic inhibition or facilitation of A-V propagation, the highly irregular ventricular activity resulting from AF cannot be predicted by simple scaling of the atrial activity.

(C) Because of randomly occurring electrotonic inhibition/facilitation and lack of scaling, the irregularity of the V-V interval (cycle length) should be relatively unchanged at any mean A-A interval. In other words, the coefficient of variation (CV = standard deviation/mean cycle) should be constant at varying ventricular rates.

(D) VVI pacing of the right ventricle at the appropriate frequency should lead to blockade of nearly all anterograde (i.e., A-V) impulses. The essential feature here is that the retrograde impulse invading the AVN cell is also followed by a period of refractoriness and by a slowly recovering excitability (V-A propagation curve). Obviously, the V-A curve is affected by atrial impulses in a similar manner as that described above for the A-V curve.^{40,41}

(E) During AF, an induced ventricular extrasystole should be followed by a pause that is terminated by the next anterogradely conducted V response. The pause should always be longer than the average V-V interval in the absence of ventricular extrasystoles. The latter corresponds to the so-called "compensatory pause" of AF.^{42,43}

As demonstrated in the following section, all above predictions have been borne out by the model results.

Testing the Predictions

In this section, we present results of simulations using a slightly more elaborate linear model of AVN propagation. The new ("nine-cell") model incorporates a linear array of nine cells separated into three different regions. The first region of two cells represented the atrium; the second region consisted of five cells representing the AVN; and the third region consisted of two cells representing the ventricle. Cells were connected by appropriate coupling resistances (20 k Ω), which resulted in AV conduction characteristics that were qualitatively similar to those of the black-box (three-cell) model. The nine-cell model established somewhat more realistic conditions when it came to testing all the above predictions.

(1) *The mean V-V interval increases as mean A-A interval decreases.* In Figure 6 we present simulation results in the nine-cell model demonstrating an inverse relationship between mean V-V interval and mean A-A interval during AF. The graphs in panels a and b are representative A-A interval histograms at two different mean A-A intervals (panel a, 197.3 msec; panel b, 283.5 msec) and the graphs in panels c and d are the V-V interval histograms (c, 598.7 msec; d, 532.5 msec) that correspond to panels a and b, respectively. In panel e we present a summary of five simulations in which we determined the mean V-V interval as a function of the mean A-A interval.

Overall, there was an inverse curvilinear relationship between the input rate into the AVN and the output rate to the ventricle. Indeed, since electrotonic inhibition increases the probability of AVN blockade during fibrillation, an increase in the frequency of atrial impulses entering the AVN cell results in a decrease in the mean frequency of impulses reaching the ventricles. These results provide a direct explanation to the original suggestion by Moe and Abildskov⁴⁴ that the degree of concealed conduction depends on the rate of AF. In addition, the data are qualitatively very similar to those of Chorro et al.,⁴⁵ who demonstrated an inverse relationship between atrial and ventricular rates during rapid irregular atrial pacing and during AF in the Langendorff-perfused rabbit heart. In those experiments, reduction of the AF frequency by lowering the temperature of the atrium led to an increase in the average ventricu-

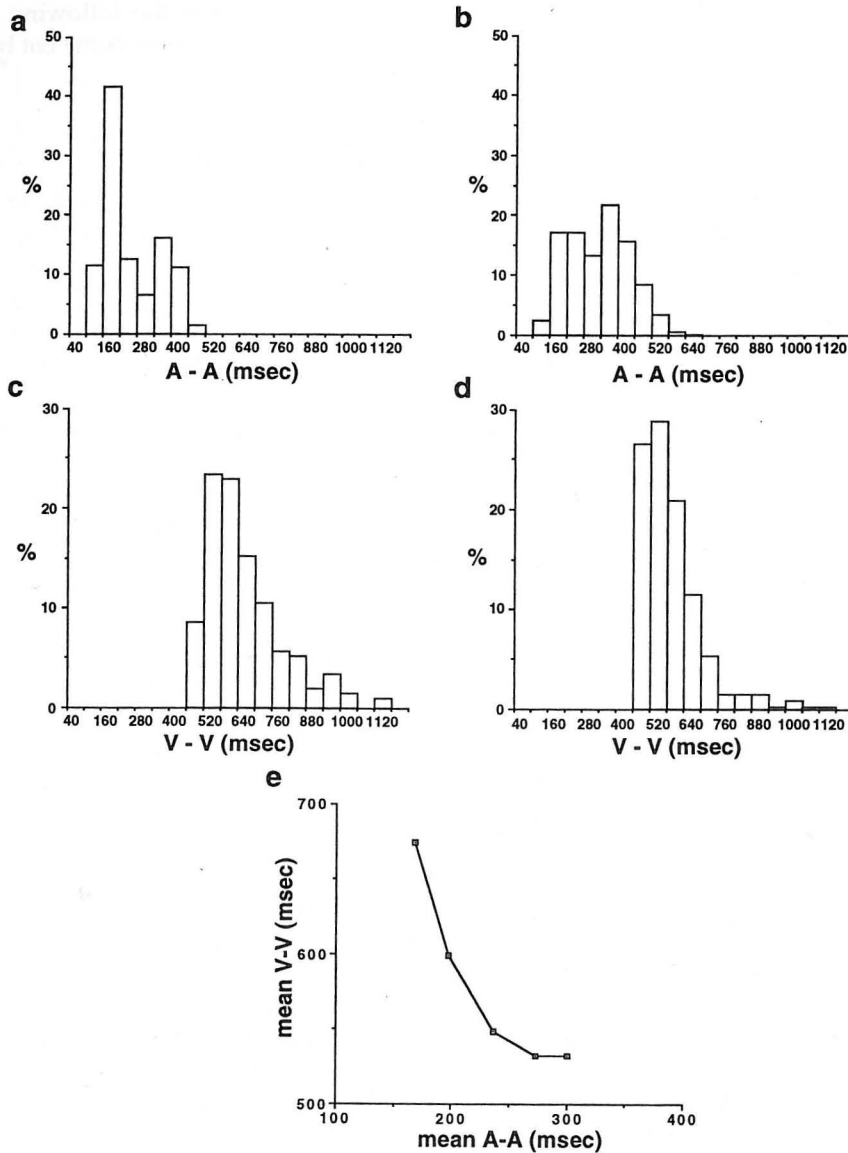


Figure 6. Panels *a* and *b*: Histograms of typical A-A distributions (nine-cell model). Panels *c* and *d*: Corresponding V-V histograms. Panel *e*: Mean V-V intervals are plotted against mean A-A intervals to show the inverse relationship. In this and other figures, electrical activity during fibrillation was simulated by driving the atrium at a random cycle length. We produced a random variable CL, which was linearly related to a Poisson distribution to give us the degrees of freedom to change the mean μ , the standard deviation s , and the minimum value for the cycle length CL_0 . Using the properties of linear transformation of random variables, one can easily verify that a random variable w following a Poisson distribution of mean W given by $W = ((CL - CL_0)(\mu - CL_0))/s^2$ is related to the random variable CL by the relation $w = ((CL - CL_0)(\mu - CL_0))/s^2$. A sample of 1000 events (or cycle lengths in the variable w domain) was extracted from a population following a Poisson distribution by using a transformation method.^{57,58} This method requires one to integrate the distribution law. We performed it numerically and used cubic splines to represent the resulting function. That representation enabled us to easily invert the cumulative probability function needed for the transformation method.

lar rate. According to the model results, increasing the mean A-A interval decreases electrotonic inhibition in preventing propagation of consecutive impulses. This leads to a lower probability of blockade at the AVN cell, since a lesser number of subthreshold depolarizations exerts lesser

effects on the ERP for the succeeding impulse. Consequently, the mean V-V interval goes down.

(2) *The V-V intervals change randomly.* We determined the statistical properties of the V-V interval in our nine-cell model of AVN propagation during AF. First, to demonstrate that the resulting

ventricular rhythm is indeed random, we constructed serial autocorrelograms (SAC) of the A-A and V-V intervals during AF. As discussed in detail elsewhere,^{12,46} the SAC is obtained by correlating each interval with itself, then with the immediately succeeding interval and subsequently with intervals ahead. It is thus possible to compute the SAC coefficients R_i of the interval sequence in question using the following equation (see also reference 59):

$$R_i = \frac{1}{N - (i + 1)} \times \sum_{j=0}^{N-(i+1)} \frac{(CL_j - \mu)(CL_{j+i} - \mu)}{\sigma_x \sigma_y} \quad (1)$$

where

$$\mu = \frac{1}{N} \sum_{j=0}^{N-1} CL_j \quad (2)$$

N represents the number of V-V intervals in the sequence, CL is the duration of the V-V interval or cycle length, μ is the mean V-V interval, and σ_x and σ_y are the variances of the sequences x and y . Each coefficient R_i gives the degree of correlation between a sequence of V-V intervals (x) and a similar sequence (y) occurring i impulses later.

It is clear from Figure 7 that both the A-A (panel a) and the V-V interval (panel b) are essentially uncorrelated. Indeed, in each case, all R_i 's > 0 have values that are statistically not significantly different from 0. Thus, the simulations demonstrate that when a random atrial input is used to simulate AF, the resulting V-V intervals are also random. Yet, it is important to note that, as demonstrated in Figure 8, the relative frequency of occurrence of V-V intervals of different lengths is essentially independent of the specific distribution of the A-A intervals. In the example shown in Figure 8a, the A-A interval varies randomly according to a skewed distribution, whereas in b, the distribution is more symmetrical. However, in each case, the shape of V-V distribution is different from the shape of A-A distribution. These results are robust and clearly demonstrate that in this nine-cell model, the V-V interval during AF is not the result of simple scaling of A-A intervals.

(3) *The coefficient of variation.* In a previous publication, Wittkamp et al.^{23,35} demonstrated that one of the basic characteristics of the ventricular rhythm in patients with AF is the maintenance of its "irregularly irregular" nature at wide ranges of

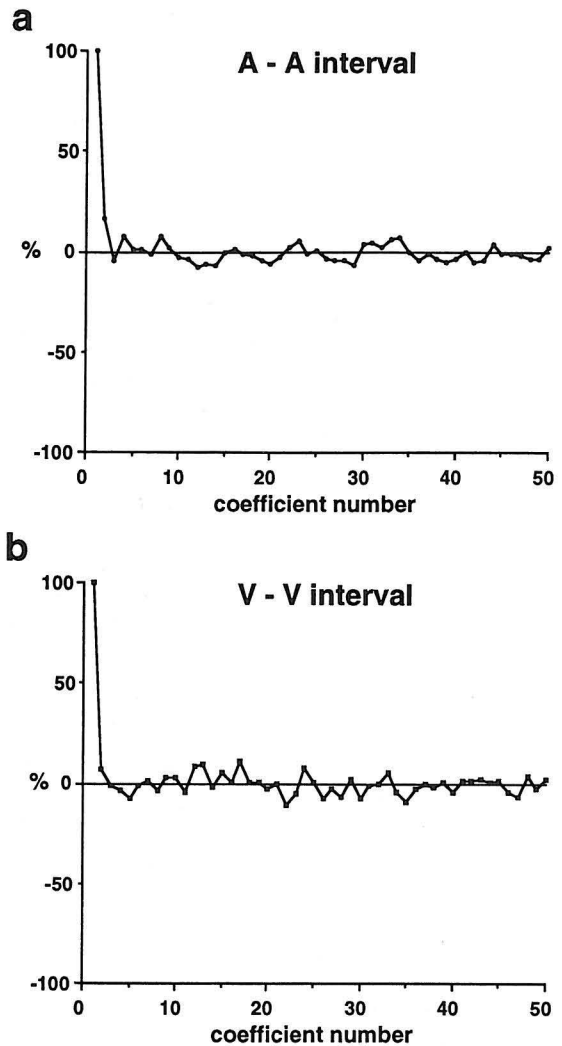


Figure 7. Panel a: Serial autocorrelogram (SAC) of A-A intervals in a typical run. Panel b: Corresponding SAC of V-V intervals. See text for details.

mean R-R intervals. Typically, the R-R interval histogram is broad with a coefficient of variation ($CV = s/\mu$) in the order of 0.23. Thus, additional evidence in support of the idea that the irregular ventricular rhythm observed in our simulations cannot be attributed to simple scaling of the atrial rhythm was sought in determinations of the CV of the V-V intervals under varying conditions.⁴⁷ The data presented in Figure 9 were obtained from simulations of AF using the nine-cell model at seven different mean A-A intervals. In panel a, we have plotted the standard deviation as a function of the mean V-V interval. In panel b, we have plotted the coefficient of variation, also as a function of the V-V interval. The results show that while the standard deviation increases linearly with the mean V-

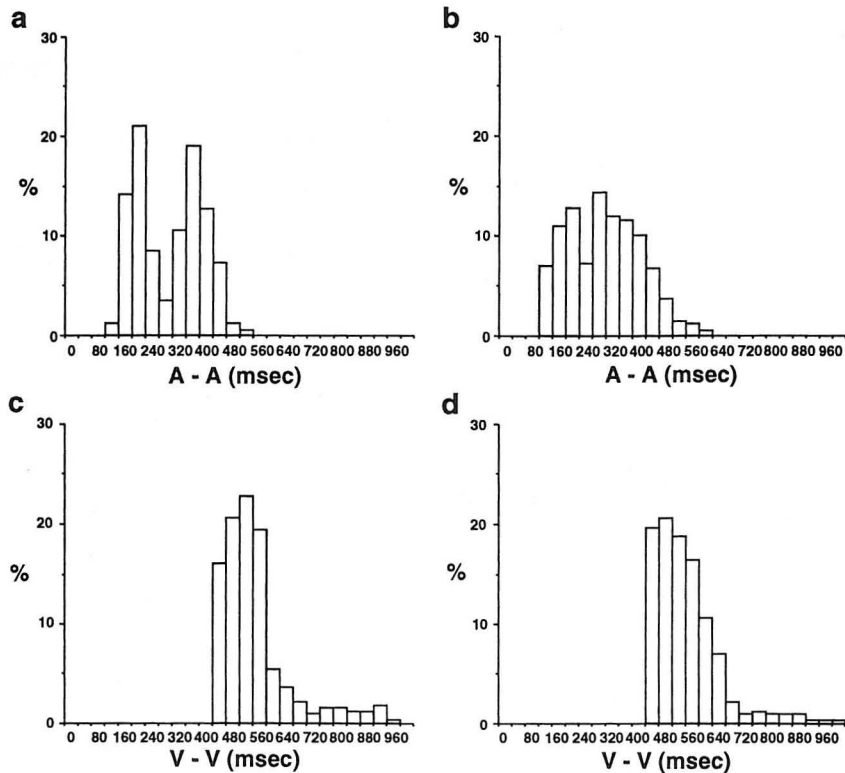


Figure 8. Panels a and b: Two different A-A distributions with similar mean A-A intervals (271 and 275 msec). Panels c and d: Corresponding V-V intervals. Note the similar shapes of the ventricular distributions.

V interval, the coefficient of variation remains relatively unchanged between 0.20 and 0.25, demonstrating that the relative variability of the ventricular rhythm during AF remains approximately constant, irrespective of the mean V-V interval. These modeling data reproduce closely the clinical results of Wittkamp et al.^{23,35} and further strengthen the idea that the mechanism of the irregularly irregular ventricular rhythm during AF is the result of electrotonic modulation at the level of the AVN.

(4) *VVI pacing.* The observation that right ventricular pacing at cycle lengths appreciably longer than the shortest R-R interval during AF is able to capture all anterograde impulses⁴⁰ may be explained also in terms of concealed conduction and electrotonic inhibition. The idea here is that each impulse of ventricular origin that propagates retrogradely through the AVN should reset its refractory period and impair propagation of immediately succeeding impulses of atrial origin. On the other hand, those impulses of ventricular origin that block within the AVN should produce electrotonic inhibition and delay propagation of atrial impulses that succeed them. The end result would be a reduction of the safety factor for anterograde conduction, which may explain why the number

of short R-R intervals diminishes even at VVI pacing rates that do not cause complete anterograde block. These simulations require repetitive ventricular stimulation, and, therefore, one must use the nine-cell model to prevent the ventricular stimulus itself from interfering with AV conduction.

In Figure 10, we present results obtained when the nine-cell model was used to study the effects of ventricular pacing at decreasing pacing intervals during AF. Coupling conditions were similar to those of the three-cell model with the exception that, in the larger array, coupling resistances were reduced to 20 k Ω to allow for a total AV conduction time of 70 msec. In panel a, AF at a mean A-A interval of 329 msec resulted in a mean V-V interval of 558 msec. The interval plot shows successive V-V intervals obtained in the nine-cell array before (first 150 cycles) and during ventricular pacing using a VVI pacemaker protocol. Pacing intervals were changed in a step-wise manner from 600 to 500, 475, and 450 msec. In accordance with results in patients suffering from AF,⁴⁰ at the pacing interval of 600 msec, all V-V intervals longer than 600 msec were abolished, and there was a slight decrease in the number of intervals shorter than 600 msec. This be-

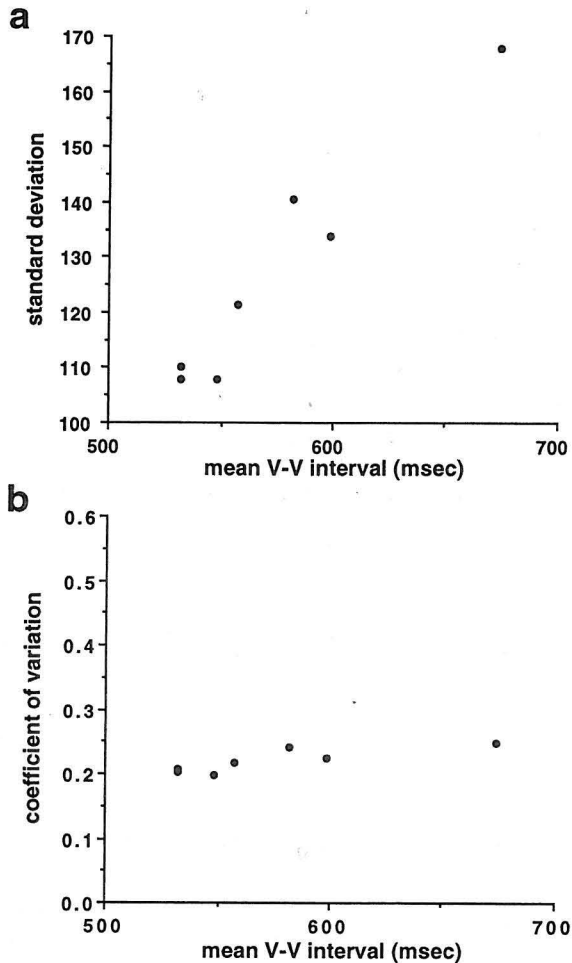


Figure 9. Panel a: Standard deviations of V-V intervals resulting from seven different mean A-A stimulation protocols plotted against mean V-V intervals. Panel b: Coefficient of variation plotted as a function of mean V-V intervals. The standard deviation varies linearly with the mean, while the coefficient of variation stays approximately constant.

came more clearly apparent at 500 and 475 msec. At 450 msec, > 95% of intervals were captured by VVI pacing, even though the minimal V-V interval ($V-V_{\min}$) during AF was 420 msec. These results are in agreement with patient data obtained by Wittkamp et al.⁴⁰ but demonstrate that resetting of AVN pacemaker activity is not needed to explain elimination of short V-V intervals by ventricular pacing at relatively long cycle lengths. However, a critical comparison of the data in panel a with clinical results (see Fig. 9 in Meijler and Wittkamp²³) reveals that, while in the clinical results all R-R intervals were abolished when the difference between the VVI cycle length (CL_{VVI}) and the minimum R-R interval during AF was slightly larger than 200 msec, in the simu-

lations > 95% of V-V intervals could be captured only when the difference between CL_{VVI} and $V-V_{\min}$ was reduced to 40 msec (see Fig. 10a).

Recently, Vereckei et al.⁴⁸ used a dog model to demonstrate that the difference between the ventricular pacing cycle length resulting in > 95% ventricular captures and the shortest spontaneous R-R interval during AF and atrial flutter is a linear function of the shortest spontaneous R-R interval during atrial flutter and AF. This suggests that if conditions are set in the model to increase the mean V-V interval, the $V-V_{\min}$ at which > 95% of V-V intervals are captured should also increase. This is precisely what happens, as illustrated in panel b of Figure 10. In these simulations, the mean A-A interval was decreased to 168 msec, which, as expected (see Fig. 6), resulted in an increased mean V-V interval of 674 msec. Under these conditions, VVI pacing at decreasing cycle lengths led to progressively more captures of long as well as short V-V intervals until, at 500 msec, all anterograde transmission was blocked despite the fact that the pacing intervals were much longer than the shortest V-V intervals in the absence of pacing. These results compare very well with those obtained by Wittkamp et al.⁴⁰ in patients. Moreover, analysis of the individual cell responses (not shown) provides a mechanistic explanation for the capture of short as well as long V-V intervals by VVI pacing: the essential feature here was that the retrograde impulse invading the AVN cells was followed by refractoriness with slow recovery of excitability, setting the stage for electrotonic inhibition of anterograde impulses.

(5) *The "compensatory pause" of AF.* The above explanation applies also to the so-called compensatory pause of AF.^{42,43} For many years, it has been known that the ventricular cycle is lengthened following a ventricular extrasystole even in the presence of AF. The phenomenon was attributed by Langendorf and Pick⁴² to lengthening of the AVN refractory period, as a result of concealed retrograde conduction of the ventricular extrasystole into the AVN. In a more recent publication, Wittkamp et al.⁴¹ demonstrated that premature ventricular stimuli (S) at a constant interval after the R wave (RS) of 660 msec caused the histogram of the poststimulus (SR) interval to shift 300 msec to the right. However, the histogram of the SR interval did not differ statistically from the histogram of the R-R interval in the absence of stimuli. Wittkamp et al.⁴¹ attributed this interesting phenomenon to resetting of AVN pacemaker activity by the retrograde impulse of ventricular

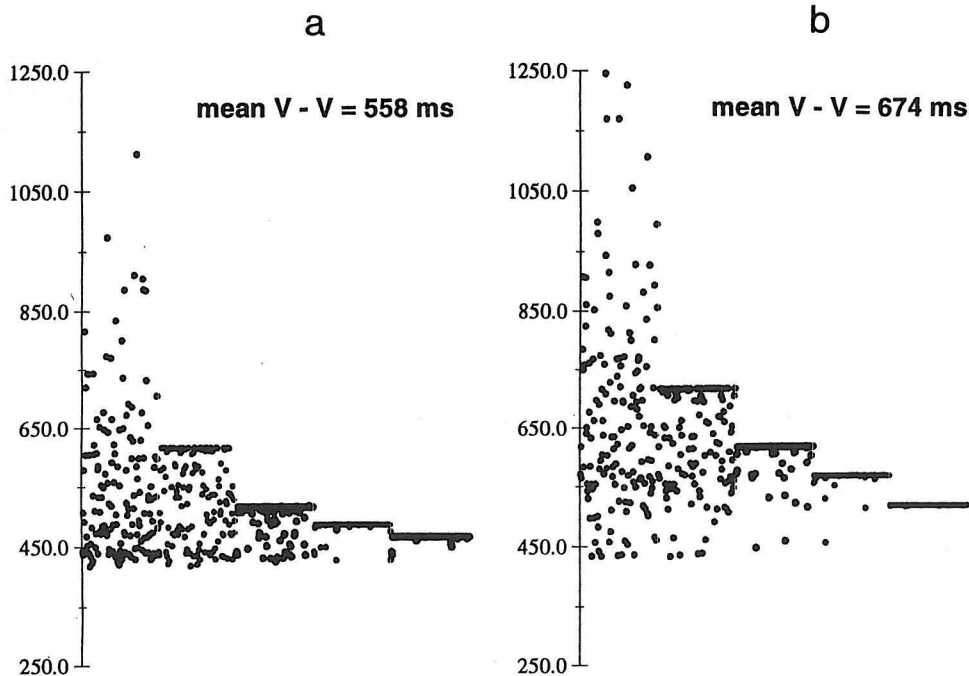


Figure 10. Panel a: One hundred fifty successive V-V intervals (mean V-V = 558 ms), plotted against cycle number followed by the same atrial stimulation protocol with VVI pacing at 600-, 500-, 475-, and 450-ms cycles. Panel b: A similar run with mean V-V cycle length of 674 ms and VVI pacing at 700-, 600-, 550-, and 500-ms cycles.

origin. On the other hand, our model results suggest the equally plausible explanation that the retrograde impulse invading the AVN cells “reset” their refractory period. This sets the stage for electrotonic inhibition of the immediately succeeding anterograde impulses with prolongation of the SR interval. In Figure 11, we have plotted the results obtained in a simulation in which a ventricular pacing stimulus (S) was applied at a constant V-S interval of 500 msec. Panel a shows the V-V interval histogram and panel b shows the mean S-V interval. Similar to what has been shown to occur in patients with AF, the ventricular extrasystole caused the S-V histogram to shift 104.9 msec to the right without dramatically changing its shape. Once again, these results support the applicability of the model to the understanding of AVN function during AF.

Anterograde Block During Ventricular Pacing

In their article, Watanabe and Watanabe¹ strongly defend the decremental conduction concept in explaining the rate and rhythm of the ventricular responses during AF. However, as discussed above, there are important flaws in the contention that decremental AVN conduction explains concealment of atrial impulses even

when they propagate through fully recovered AVN tissue. Similarly, decremental conduction cannot account for the effects of VVI pacing demonstrated in patients with AF⁴⁰ as well as in the model (see Figs. 10 and 11), unless the term is being used solely for descriptive purposes with no mechanistic intent. Returning to Figure 3 in the article by Watanabe and Watanabe,¹ it is there postulated that two alternative scenarios may explain the elimination of shorter R-R intervals by right ventricular pacing during AF. The first one is based on the idea that the R-R interval from an impulse initiated in the ventricle to the following conducted QRS should be longer than the refractory period of the node, by the sum of retrograde and forward His-Purkinje conduction times. In the second scenario, the Watanabes¹ speculate that intranodal conduction “often decrements and is concealed even after expiration of the AVN refractory period.” On the basis of this idea and with no demonstrative evidence to support it, they further suggest that blockade of atrial impulses during ventricular pacing is predominantly dependent on decremental conduction rather than AVN refractoriness. Although our results are in agreement with the first Watanabe scenario, they are in complete disagreement with their second speculation. In fact, our simulation results

Digitalis and Quinidine in AF

In this section, we present a brief discussion of the applicability of our model in explaining the effects of drugs known to influence the ventricular response in patients with ventricular fibrillation. We concentrate on the effects of digitalis and quinidine because the reasoning used for these two drugs is almost certainly applicable for several other drugs as well.

The traditional explanation for the effects of digitalis on the ventricular rate during AF is that the drug slows AVN conduction, in part through a decrease in the upstroke velocity of the action potential of the "AV nodal cell," and in part through a prolongation of the AVN refractory period.⁴⁹ Such an explanation does not take into consideration that therapeutic doses of digitalis do not appreciably lengthen the PR interval in patients with sinus rhythm, although it may be assumed that during exercise (high sinus rates), shortening of PR interval is less than would be the case in the absence of digitalis. The above explanation also does not consider that digitalis significantly abbreviates action potential duration and refractory period of the atrial myocardium.^{50,51} The latter effect is exemplified by the fact that atrial flutter often converts into AF in the presence of digitalis. Both the prolongation of AVN refractory period at high atrial rates and the abbreviation of the atrial refractory period would act in concert to reduce the ventricular rate during AF. Yet, it is important to note that the latter effect alone would be sufficient to explain the slowing of the ventricular rate induced by digitalis. This is because more atrial impulses would bombard the AVN per unit time as a result of the increase in the mean frequency of fibrillation. As demonstrated by our model results (see Fig. 4), this would increase the role of electrotonic inhibition in preventing propagation of consecutive impulses. Thus, electrotonic inhibition of conduction would lead to a greater probability of blockade since the subthreshold depolarization induced by each concealed atrial impulse would tend to shift the AVN conduction curve for the succeeding impulse a little more to the right. Once again, the results of the model strongly support this idea in that they demonstrate that during simulated AF there is an inverse relationship between the A-A interval and the V-V interval (see Fig. 6).

The action of quinidine would be opposite to that of digitalis. In the absence of autonomic innervation, the quinidine-induced prolongation of atrial refractory period⁵² would act to abbreviate

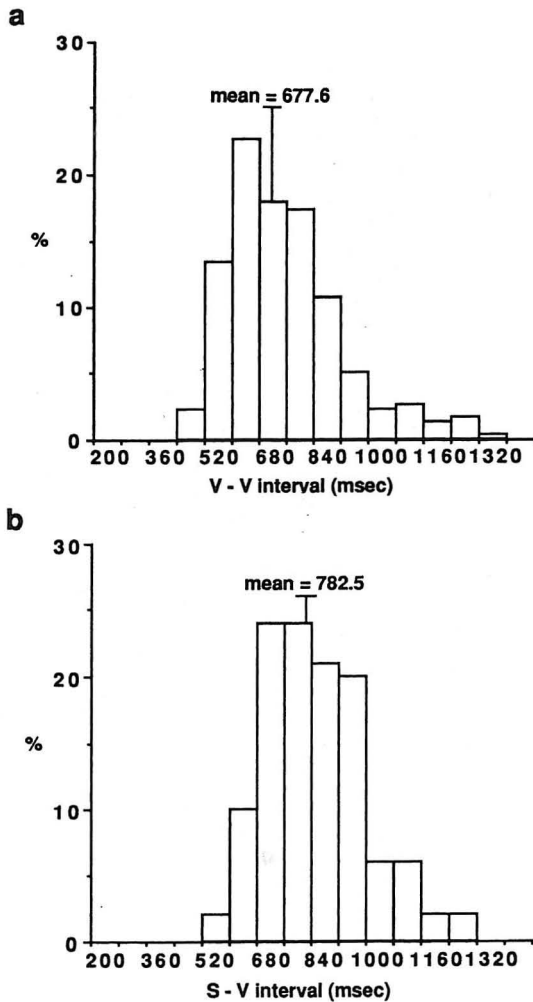


Figure 11. Panel a: Histogram of spontaneous V-V intervals. Panel b: Histogram of "escape interval" after a properly timed ventricular pacing stimulus (S-V interval). The two histograms are similar in shape, but the mean S-V interval is longer (782.5 msec) than the mean V-V interval (677.8 msec).

provide strong evidence in support of the idea that it is AVN refractoriness and its modulation by discrete electrotonic depolarizations of atrial origin that explain the phenomena in question. Indeed, during ventricular pacing in the model, the AVN region is excited retrogradely by a ventricular impulse. This is followed by a refractory period that is then lengthened by electrotonic inhibition of repetitive subthreshold atrial impulses. In other words, retrograde excitation of the AVN resets the AV conduction curve to the right, which sets the stage for concealment of anterograde impulses and electrotonic modulation of subsequent events.

the R-R interval through a slowing of the mean atrial fibrillatory rate. However, in intact, innervated hearts, the anticholinergic effect of quinidine may variably affect the outcome, depending on the underlying vagal tone.⁵³ In general, however, quinidine would diminish the number of available atrial impulses that can reach the AVN during AF. Less atrial impulses would produce less electrotonic inhibition, and possibly would lead to more opportunity for summation and to an increase of the safety factor for propagation. Thus, the propagation curve would be shifted slightly to the left for some impulses traversing the AVN, resulting in the clinically well-known increase in ventricular rate, when one tries to restore sinus rhythm by using quinidine in patients with AF.

Conclusions

- (1) Electrotonic modulation of AVN propagation is compatible with the concept of concealed conduction in the AVN.
- (2) Electrotonic modulation of AVN excitability by repetitive atrial impulses is a viable explanation for the characteristics of the ventricular response in patients with AF.
- (3) Decremental conduction cannot be operative during AF.
- (4) Computer simulations suggest that the mechanism of electrotonic modulation of AVN propagation indeed satisfies most if not all ventricular response characteristics during AF.

Acknowledgments: José Jalife and Frits Meijler wish to thank Jaime and Olga Jalife for the use of their home in Cuernavaca during the initial writing of this paper. We thank also Dr. Jan Strackee from the University of Amsterdam for his help in the statistical analyses.

References

1. Watanabe Y, Watanabe M: Impulse formation and conduction of excitation in the atrioventricular node. *J Cardiovasc Electrophysiol* 1994;5:517-531.
2. Hoffman BF, Cranefield PF: *Electrophysiology of the Heart*. McGraw-Hill, New York, 1960, p. 156.
3. Katholi CR, Urthaler F, Macy J, et al: A mathematical model of automaticity in the sinus node and AV junction based on weakly coupled relaxation oscillators. *Comp Biomed Res* 1977;10:529-543.
4. Meijler FL, Fisch C: Does the atrioventricular node conduct? *Br Heart J* 1989;61:309-315.
5. Rosenblueth A: Functional refractory period of cardiac tissues. *Am J Physiol* 1958;194:171-183.
6. Jalife J: The sucrose gap preparation as a model of AV nodal transmission: Are dual pathways necessary for reciprocation and AV nodal "echoes"? *PACE* 1983;6:1106-1122.
7. Antzelevitch C, Moe GK: Electrotonic inhibition and summation of impulse conduction in mammalian Purkinje fibers. *Am J Physiol* 1983;245:H42-H53.
8. Liu Y, Zeng W, Delmar M, et al: Ionic mechanisms of electrotonic inhibition and concealed conduction in rabbit atrioventricular nodal myocytes. *Circulation* 1993;88:1634-1646.
9. Engelmann ThW: Beobachtungen und Versuche an suspendierten Herzen. *Pflügers Arch* 1894;56:149-202.
10. Langendorf R: Concealed A-V conduction: The effect of blocked impulses on the formation and conduction of subsequent impulses. *Am Heart J* 1948;35:542-552.
11. Fisch C: *Electrocardiography of Arrhythmias*. Lea & Febiger, Philadelphia, 1990, p. 1.
12. Bootsma BK, Hoelen AJ, Strackee J, et al: Analysis of the R-R intervals in patients with atrial fibrillation at rest and during exercise. *Circulation* 1970;41:783-794.
13. Brody DA: Ventricular rate patterns in atrial fibrillation. *Circulation* 1970;41:733-735.
14. Scherf D, Schott A: *Extrasystoles and Allied Arrhythmias*. 2nd edition. William Heinemann Medical Books, Ltd, Chicago, 1973, p. 561.
15. Hoffman BF: Electrical activity of the atrio-ventricular node. In Paes de Carvalho A, de Mello WC, Hoffman BF, eds: *The Specialized Tissues of the Heart*. Elsevier, Amsterdam, 1961, pp. 143-158.
16. Paes de Carvalho A, de Almeida DF: Spread of activity through the atrioventricular node. *Circ Res* 1960;8:801-809.
17. Zipes DP, Mendez C, Moe GK: Some examples of Wenckebach periodicity in cardiac tissues with an appraisal of mechanisms. In Rosenbaum MB, Elizari MV, eds: *The Frontiers of Cardiac Electrophysiology*. Martinus Nijhoff, Amsterdam, 1983, pp. 357-375.
18. West TC, Toda N: Response of the A-V node of the rabbit to stimulation of intracardiac cholinergic nerves. *Circ Res* 1967;20:18-31.
19. Mazgalev T, Dreifus LS, Michelson EL: A new mechanism for atrioventricular nodal gap-vagal modulation of conduction. *Circulation* 1989;79:417-430.
20. Billette J: Atrioventricular nodal activation during premature stimulation of the atrium. *Am J Physiol* 1987;252(Heart Circ Physiol 21):H163-H177.
21. Jalife J, Moe GK: Excitation, conduction, and reflection of impulses in isolated bovine and canine cardiac Purkinje fibers. *Circ Res* 1981;49:233-247.
22. Merideth J, Mendez C, Mueller WJ, et al: Electrical excitability of atrioventricular nodal cells. *Circ Res* 1968;23:69-85.
23. Meijler FL, Wittkamp FHM: Role of the atrioventricular node in atrial fibrillation. In Falk RH, Podrid PJ, eds: *Atrial Fibrillation: Mechanisms and Management*. Raven Press, Ltd., New York, 1992, pp. 59-80.
24. Mendez C, Moe GK: Demonstration of a dual A-V nodal conduction system in the isolated rabbit heart. *Circ Res* 1966;19:378-393.

25. Wennemark JR, Bandura JP, Brody MD, et al: Micro-electrode study of high grade block in canine Purkinje fibers. *J Electrocardiol* 1975;8:299-306.
26. Jalife J, Moe GK: Effect of electrotonic potentials on pacemaker activity of canine Purkinje fibers in relation to parasytostole. *Circ Res* 1976;39:801-808.
27. Prystowsky EN, Zipes DP: Inhibition in the human heart. *Circulation* 1983;68:707-713.
28. Oreto G, Satullo G, Luzzo F, et al: Electrotonic inhibition of an idioventricular escape focus by nonconducted sinus impulses. *Am Heart J* 1988;116:1097-1099.
29. Verrier RL, Brooks WW, Lown B: Protective zone and the determination of vulnerability to ventricular fibrillation. *Am J Physiol* 1978;234:H592-H596.
30. Allesie MA, Bonke, FIM, Schopman FJG: Circus movement in rabbit atrial muscle as a mechanism of tachycardia. III. The "leading circus" concept: A new model of circus movement in cardiac tissue without the involvement of an anatomical obstacle. *Circ Res* 1977;41:9-18.
31. Davidenko JM, Delmar M, Lorente P, et al: Electrotonic inhibition and active facilitation of excitability in ventricular muscle. *J Cardiovasc Electrophysiol* 1994;5:945-960.
32. Luo C, Rudy Y: A model of the ventricular cardiac action potential. *Circ Res* 1991;68:1501-1526.
33. Meijler FL, Janse MJ: Morphology and electrophysiology of the mammalian atrioventricular node. *Physiol Rev* 1988;68:608-647.
34. James TN: Structure and function of the AV junction. *Jpn Circ J* 1983;47:1-47.
35. Wittkampf FHM, Robles de Medina EO, Strackee J, et al: Scaling in atrial fibrillation? In Wittkampf FHM, ed: *Atrioventricular Nodal Transmission in Atrial Fibrillation*. Ph.D. Thesis, State University Utrecht, The Netherlands, 1991, pp. 89-104.
36. Talajic M, Papadatos D, Villemarie C, et al: A unified model of atrioventricular nodal conduction predicts dynamic changes in Wenckebach periodicities. *Circ Res* 1991;68:1280-1293.
37. Heethaar RM, Denier van der Gon JJ, Meijler FL: A mathematical model of AV conduction in the rat heart I. *Cardiovasc Res* 1973;7:105-114.
38. Heethaar RM, De Vos Burchart RM, Denier van der Gon JJ, et al: A mathematical model of AV conduction in the rat heart II. *Cardiovasc Res* 1973;7:542-556.
39. Denes P, Wu D, Dhingra RC, et al: Dual AV nodal pathways. A common electrophysiological response. *Br Heart J* 1975;37:1069-1076.
40. Wittkampf FHM, De Jongste MJL, Lie KI, et al: Effect of right ventricular pacing on ventricular rhythm during atrial fibrillation. *J Am Coll Cardiol* 1988;11:539-545.
41. Wittkampf FHM, De Jongste MJL, Meijler FL: Competitive anterograde and retrograde atrioventricular junctional activation in atrial fibrillation. *J Cardiovasc Electrophysiol* 1990;1:448-456.
42. Langendorf R, Pick A: Artificial pacing of the human heart: Its contribution to the understanding of the arrhythmias. *Am J Cardiol* 1971;26:516-525.
43. Pritchett LC, Smith WM, Klein SJ, et al: The "compensatory pause" of atrial fibrillation. *Circulation* 1980;62:1021-1025.
44. Moe GK, Abildskov JA: Observations on the ventricular dysrhythmia associated with atrial fibrillation in the dog heart. *Circ Res* 1964;14:447-460.
45. Chorro FJ, Kirchhof CJHJ, Brugada J, et al: Ventricular response during irregular atrial pacing and atrial fibrillation. *Am J Physiol* 1990;259:H1015-H1021.
46. Cohen RJ, Berger RD, Dushane TE: A quantitative model for the ventricular response during atrial fibrillation. *IEEE Trans Biomed Eng BME* 1983;30:769-780.
47. Kirsch JA, Sahakian AV, Baerman JM, et al: Ventricular response to atrial fibrillation: role of atrioventricular conduction pathways. *J Am Coll Cardiol* 1988;12:1265-1272.
48. Vereckei A, Vera Z, Pride HP, et al: Atrioventricular nodal conduction rather than automaticity determines the ventricular rate during atrial fibrillation and atrial flutter. *J Cardiovasc Electrophysiol* 1992;3:534-543.
49. Hoffman BF, Bigger JT Jr: Digitalis and allied cardiac glycosides. In Goodman Gilman A, Rall TW, Nies AS, et al, eds: *The Pharmacologic Basis of Therapeutics*. 8th edition. Pergamon Press, New York, 1990, pp. 814-839.
50. Hoffman BF, Singer DH: Effects of digitalis on electrical activity of cardiac fibers. *Prog Cardiovasc Dis* 1964;7:226-260.
51. Meijler FL: An "account" of digitalis and atrial fibrillation. *J Am Coll Cardiol* 1985;5:A60-A68.
52. Goldman MJ: Quinidine treatment of auricular fibrillation. *Am J Med Sci* 1951;186:382-391.
53. Stanton MS: Class I antiarrhythmic drugs: Quinidine, procainamide, disopyramide, lidocaine, mexiletine, tocainide, phenytoin, moricizine, flecainide, propafenone. In Zipes DP, Jalife J, eds: *Cardiac Electrophysiology: From Cell to Bedside*. 2nd edition. WB Saunders, Philadelphia, 1995, pp. 1296-1317.
54. Matsuura H, Ehara T, Omoto T: An analysis of the delayed outward current in single ventricular cells of the guinea pig. *Pflügers Arch* 1987;410:596-603.
55. Hoshino K, Anumonwo J, Delmar M, et al: Wenckebach periodicity in single atrioventricular nodal cells from the rabbit heart. *Circulation* 1990;82:2201-2216.
56. Yanagihara K, Noma A, Irisawa H: Reconstruction of sino-atrial node pacemaker potential based on the voltage clamp experiments. *Jpn J Physiol* 1980;30:841-857.
57. Gear W: *Numerical Initial Value Problems in Ordinary Differential Equations*. Prentice-Hall Inc, Englewood Cliffs, 1971.
58. Press W, Flannery BP, Teukolsky SA, et al: *Numerical Recipes*. Cambridge University Press, New York, 1986.
59. Kreyszig E: *Introductory Mathematical Statistics*. John Wiley & Sons, New York, 1970, pp. 335-336.